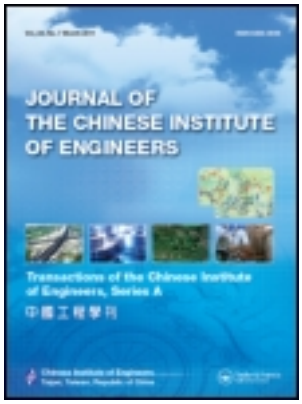

Journal of the Chinese Institute of Engineers
Publication details, including instructions for authors and subscription information:
http://www.tandfonline.com/loi/tcie20

Design of a multi-layer fuzzy logic controller using pole assignment for bipedal walking at varying speeds

Kuo-Yang Tu [a] [b] & Tsu-Tian Lee [c]

[a] Department of Electronic Engineering , Lunghwa University of Science and Technology , Taoyuan, Taiwan, 333, R.O.C

[b] Graduate Institute of System and Control Engineering , National Kaohsiung First University of Science and Technology , Kaohsiung, Taiwan, 811, R.O.C. Phone: 886-7-6011000 ext. 2810; Fax: 886-7-6011000 ext. 2810; E-mail:

[c] Department of Electrical and Control Engineering , National Chiao Tung University , Hsinchu, Taiwan, 300, R.O.C.

Published online: 04 Mar 2011.

To cite this article: Kuo-Yang Tu & Tsu-Tian Lee (2004) Design of a multi-layer fuzzy logic controller using pole assignment for bipedal walking at varying speeds, Journal of the Chinese Institute of Engineers, 27:1, 55-68, DOI: 10.1080/02533839.2004.9670849

To link to this article: http://dx.doi.org/10.1080/02533839.2004.9670849

DESIGN OF A MULTI-LAYER FUZZY LOGIC CONTROLLER USING POLE ASSIGNMENT FOR BIPEDAL WALKING AT VARYING SPEEDS

Kuo-Yang Tu* and Tsu-Tian Lee

ABSTRACT

When a biped robot detects obstacles along its path, it will reduce its walking speed to change direction for obstacle avoidance. It is essential for a biped robot to be able to vary its speed during walking. To control biped robots with variable walking speed capability, a Multi-Layer Fuzzy Logic Controller (MLFLC) is developed using the pole assignment technique in this paper. This method extends the previous result, that a switching surface, whose parameters are scaling factors, exists in a Multi-Layer Fuzzy Logic Controller (Tu *et al*., 2000). In this study, the poles of a closed-loop control system are derived relative to the switching surface parameters, i.e. the normalized scaling factors. Therefore, after choosing the appropriate poles, scaling factors are determined and then a Multi-Layer Fuzzy Logic Controller is designed. This design has two important features: (1) simplifying Fuzzy Logic Controller (FLC) design to select only the scaling factors; (2) pursuing the system performance requirement, based on the pole assignment. A three-link biped robot is used as the illustrative example. Simulation results are included.

Key Words: fuzzy logic controller, biped robot, varying speed.

I. INTRODUCTION

Research on biped robots has been conducted for three decades. At first, many scientists were only engaged in theoretical studies (Frank, 1970; Vukobratovic *et al*., 1970; Frank and Vukobratovic, 1979; Gubina *et al*., 1974; Hemami and Wyman, 1979). In 1973, Kato and his colleague (Kato *et al*., 1974) designed and constructed WL-5, an eleven-degree-of-freedom biped robot to accomplish, the first walking biped robot in the world. Biped robot locomotion was realized concretely. In addition to Kato's group, other scientists have designed and implemented various kinds of biped robots (Miura and Shimoyama, 1984; Raibert, 1986; Arimoto and Miyazaki, 1984; Zheng and Sias. Jr., 1988; Shih and Gruver, 1992; Kajita *et al*., 1992; Miller, 1994; Shih and Chiou, 1998). Biped robots able to walk like humans have always been an important research topic.

Biped walking can be divided into two areas: static balance and dynamic balance. Static balance involves maintaining the Normal Projection of robot's Center of Mass (NPCM) inside a stable region, which is usually the limit defined by the contact points between the biped feet (or foot) and the ground. In static balance, the biped walks slowly to prevent the NPCM from moving outside of the stable region. Static balance imposes a gait speed constraint on biped walking. For a fast gait speed, the Zero Moment Point (ZMP), where the sum of all moments acting on the biped are equal to zero (Borovac *et al*., 1989), is defined to replace the NPCM for developing dynamically balanced walking. Dynamic balance is designed to consider the ZMP within a stable region such that

*Corresponding author. (Tel: 886-7-6011000 ext. 2810; Fax: 886-7-6011239; Email: tuky@ccms.nkfust.edu.tw)

K. Y. Tu is with the Department of Electronic Engineering, Lunghwa University of Science and Technology, Taoyuan, Taiwan 333, R.O.C and is currently with the Graduate Institute of System and Control Engineering, National Kaohsiung First University of Science and Technology, Kaohsiung, Taiwan 811, R.O.C.

T. T. Lee is with the Department of Electrical and Control Engineering, National Chiao Tung University, Hsinchu, Taiwan 300, R.O.C.

the supporting foot (or feet) can produce opposing forces to prevent the biped from falling on the ground. As a result, static balance restricts the biped robot to walking slowly, while dynamic balance permits it to walk with a fast gait. Note that in the case of static balance, the NPCM and the ZMP are located at the same point. This means that static balance is a special case of full foot contact dynamic balance (Kum and Miller, 1999).

Both statically and dynamically balanced walking has been designed for biped locomotion. During statically balanced walking, the stable region of a biped robot is the convex hull formed by one supporting foot or two supporting feet. The stable region for providing opposing forces to support the robot body is thus small. Statically balanced walking is usually applied to four- or more-legged robots such that at least three feet form a larger stable region to support the robot's body. The stability of such a multi-legged walking robot was adequately quantified by Song and Waldron (1988). However, static balance is still important in the study of a practical biped-walking robot, especially when the body needs to support a load or to move on rough terrain such as stairs or a sloping surface. Shih and Chiou designed a biped robot for statically balanced walking on an uneven floor (Shih and Chiou, 1998). Furthermore, dynamically balanced walking biped robots have been developed (Miura and Shimoyama, 1984; Kajita *et al*., 1992; Takanishi *et al*., 1985; Furusho and Sano, 1990; Grishin *et al*., 1994). More specifically, Zheng and Shen (1990) proposed a quasi-dynamic gait for a biped robot to climb a sloping surface. In contrast to static balance, dynamic balance has been widely studied in biped walking. However, in practical environments, an obstacle will force a biped robot to walk slowly for avoidance, or rough terrain will force it to adjust its step length for an adequate foothold. Thus, biped robots need to change speed during walking in practical environments. At slow speeds, the biped needs to stabilize statically during walking, while dynamic balance is required at fast speeds. As a result, both static and dynamic balance are needed for changing the gait in biped walking.

For changing gait, Hodgins and Raibert (1991) used a biped running machine to evaluate three methods for controlling step length. These three methods involve adjusting the forward running speed and the duration of the stance and flight phases. Evaluation results showed that the forward speed method gives the widest range of adjustments with good accuracy. Minakata and Hori (1994) proposed the control of the parameters of a virtual inverted pendulum for real-time speed changes for biped walking. Kum and Miller (1999) designed Cerebelar Model Arithmetic Computer (CMAC) neural networks to control a biped robot for variable-speed gaits. The control architecture contains five CMAC neural networks to take the correction in various lean postures for variable-gait speed. Such control architecture is complicated and requires much time for training the neural networks. In this paper, we propose a Multi-Layer Fuzzy Logic Control (MLFLC) to control the biped robot for varying speeds during walking. The MLFLC design intends to find a simple way to simultaneously allow both statically and dynamically balanced walking.

This paper extends the MLFLC developed in (Tu *et al*., 2000) to formularize normalized scaling factor design. It is shown that normalized scaling factors are related to the pole locations of a MLFLC system. The MLFLC design is thus reduced into selecting normalized scaling factors from characteristic functions, which are formed by pole placement. Such MLFLC design has two important features. First, the MLFLC design is reduced to selecting only its normalized scaling factors. Unlike the traditional MIMO FLC design that considers many factors, such as fuzzy sets, membership functions, linguistic rules and scaling factors, the proposed MLFLC provides a way to simplify the FLC design for MIMO systems. Second, because normalized scaling factors are selected from the pole placement, this MLFLC design is based on performance issues. This paper also extends the MLFLC design to pursue performance requirements. More specifically, as the poles are placed at a location far from the origin, the system will result in faster time response. Based on this, an MLFLC can be easily designed such that its time response simultaneously satisfies slow and fast walking gaits. Thus, the designed MLFLC also resolves the problem of control of a biped robot walking at varying gaits.

The remainder of this paper is organized as follows. The model of a three–link biped robot is introduced in section II. In section III, some preliminaries of MLFLC are introduced. The stability is analyzed in section IV. Section V is devoted to deriving the relationships between normalized scaling factors and pole locations. In section VI, a three-link biped robot system is used as the illustrative example of MLFLC design. Finally, conclusions are presented in section VII.

II. PROBLEM STATEMENT

This section first describes the dynamic model of a three-link biped robot and then formulates the problem of the biped working at varying speeds. In addition, a performance index is defined to compute the consumed energy of the biped system.

Figure 1 shows a mechanical model of a three-link biped robot. Table 1 shows the physical

Table 1 The physical dimensions of the three-link biped robot

Parameter	Length or weight
ℓ_1 (length of link 1)	0.933 m
ℓ_2 (length of link 2)	0.28 m
ℓ_3 (length of link 3)	0.933 m
m_1 (weight of link 1)	12.2 kg
m_2 (weight of link 2)	49.0 kg
m_3 (weight of link 3)	12.2 kg

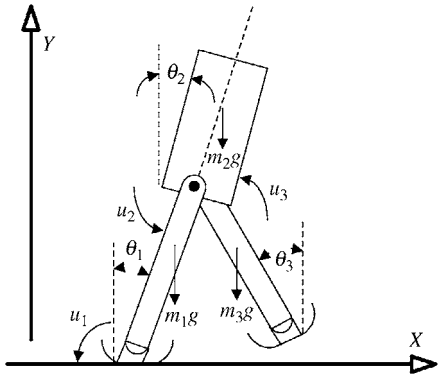

Fig. 1 Torque, force, angles and relative angles

dimensions of this biped robot. Its dynamical equation is

$$\overline{\boldsymbol{M}}(\overline{\theta})\ddot{\overline{\boldsymbol{\theta}}} = \overline{f}(\overline{\theta}, \dot{\overline{\boldsymbol{\theta}}}) + \overline{N}\overline{T} \tag{1}$$

where $\ddot{\overline{\boldsymbol{\theta}}} = [\ddot{\theta}_1 \ \ddot{\theta}_2 \ \ddot{\theta}_3]^T$, $\overline{\boldsymbol{T}} = [T_1 \ T_2 \ T_3]^T$, $\overline{M}(\cdot)$ and $\overline{N}$ are the matrices of 3×3, and $\overline{f}(\cdot)$ is the column vector of 3×1. The detailed description of the dynamical equation is given in Appendix A.

After some manipulation in Eq. (1), we have

$$\ddot{\overline{\boldsymbol{\theta}}} = \overline{\boldsymbol{M}}^{-1}(\overline{\theta})\overline{f}(\overline{\theta}, \dot{\overline{\boldsymbol{\theta}}}) + \overline{\boldsymbol{M}}^{-1}(\overline{\theta})\overline{N}\overline{T} \tag{2}$$

Let $\overline{\boldsymbol{Y}}^T = [\theta_1 \ \dot{\theta}_1 \ \theta_2 \ \dot{\theta}_2 \ \theta_3 \ \dot{\theta}_3]$. Then, (2) can be rewritten as

$$\dot{\overline{\boldsymbol{Y}}} = \overline{\boldsymbol{F}}_b(\overline{\boldsymbol{Y}}) + \overline{\boldsymbol{G}}_b(\overline{\boldsymbol{Y}})\overline{\boldsymbol{T}}_b \tag{3}$$

where $\overline{\boldsymbol{Y}} \in R^6$ describes the system state, $\overline{\boldsymbol{F}}_b(\overline{\boldsymbol{Y}}) \in R^6$, $\overline{\boldsymbol{G}}_b(\overline{\boldsymbol{Y}}) \in R^{6\times 3}$, and $\overline{\boldsymbol{T}}_b \in R^3$ are the control inputs.

The following definition is required for evaluating the system performance of the designed MLFLC.

Definition 1: For the dynamical system (3), a Performance Index is defined as

$$PI \triangleq \int \left(\frac{\overline{Y}^T Q^{6\times 6} \overline{Y}}{\left|\overline{Y}\right|_{\max}^T \left|\overline{Y}\right|_{\max}} + \frac{\overline{T}_b^T R^{3\times 3} \overline{T}_b}{\left|\overline{T}_b\right|_{\max}^T R^{3\times 3} \left|\overline{T}_b\right|_{\max}} \right) dt \tag{4}$$

where $Q^{6\times 6}$ and $R^{3\times 3}$ are the weight matrices.

Biped walking is performed by repeating a gait cycle. During a gait cycle, the biped legs are controlled to support and to move its body. Each gait cycle of the biped can be divided into four phases: (1) right-leg support phase; (2) right-leg to left-leg support exchange phase; (3) left-leg support phase; and (4) left-leg to right-leg support exchange phase. Phases (2) and (4) are also named double-support phases. A biped robot is controlled to repeat the four phases for walking.

Usually, a gait cycle is viewed as the desired walking pattern of a biped robot. The desired walking pattern is accomplished using a set of its joint trajectories. That is, if all joints are controlled to follow the set of joint trajectories, then the biped walks with the desired walking pattern. According to Lee and Liao (1988), trajectory planning in the sagittal plane can be obtained by

$$\theta_1^* = D_1 \cosh 3.094t + D_2 \sinh 3.094t \tag{5}$$

$$\theta_2^* = 0 \tag{6}$$

$$\theta_3^* = P_0 + P_1 t + P_2 t^2 + P_3 t^3 \tag{7}$$

where

$$P_0 = \theta_m$$

$$P_1 = 3.094[D_1 \sinh(3.094T_m) + D_2 \cosh(3.094T_m)]$$

$$P_2 = -(3\theta_m + 3.094C_2T_m + 2P_1T + 3P_0)/T_m^2$$

$$P_3 = (3.094C_2T_m + 2\theta_m + P_1T_m + 3P_0)/T_m^3$$

$$D_1 = -\theta_m$$

$$D_2 = \theta_m / \tanh(1.54T_m)$$

Note that θ_m denotes the maximal swing angle between the leg and the vertical in the sagittal plane, T_m denotes the period of a single-support phase, and the desired trajectory of θ_i is θ_i^*. In this research, $\theta_m = 30°$ and $T_m = 0.5$ second.

In this paper, the MLFLC design is devoted to solving the following three problems.

Problem 1: System stability.

Given the dynamic system in (3), find the sufficient conditions that guarantee the MLFLC system is

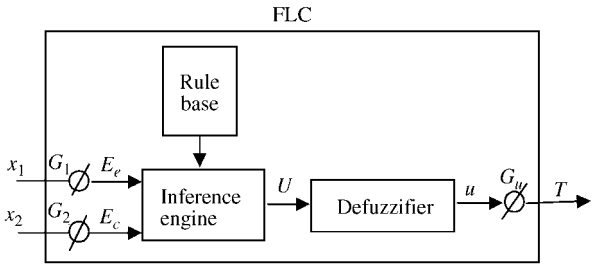

Fig. 2 A simple control scheme

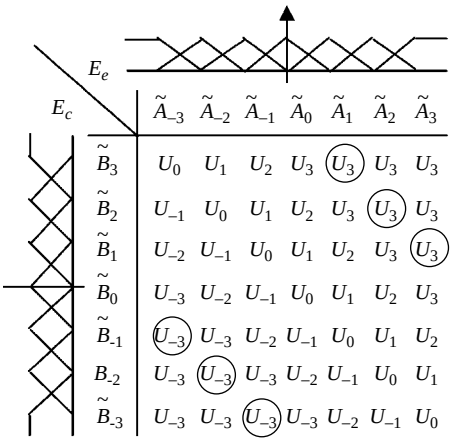

Fig. 3 The Fuzzy Suction Controller (FSC) linguistic rules

globally asymptotically stable.

Problem 2: To achieve stable walk with less PI.

A MLFLC is designed to achieve (i) fast time response and (ii) less PI.

Problem 3: Biped walking at varying speeds.

An MLFLC is designed to control the biped system for following the desired walking pattern in (5)-(7), even if T_m in (5)-(7) is varying.

III. A MULTI-LAYER FUZZY LOGIC CONTROLLER (MLFLC) AND ITS APPROXIMATED FUNCTION

In this section, some results from our previous paper (Tu *et al*., 2000; Lee *et al*., 1997) will be introduced. These results will be used to design the normalized scaling factors in an MLFLC.

The MLFLC design is based on a simple Fuzzy Logic Controller (FLC) as shown in Fig. 2. A simple FLC is a two-inputs one-output system. More specifically, its linguistic rules are designed as shown in Fig. 3, where $\tilde{A}_i$ and $\tilde{B}_i$ (for i=-3, ⋯, 0, ⋯, 3.) are the fuzzy sets for the normalized input E_e and E_c, respectively, and U_i (for i=-3, ⋯, 0, ⋯, 3) is the control action of the FLC. As shown in Fig. 3, the diagonal control actions U_0 are arranged like a switching line in a suction controller. The control actions paralleling U_0 are arranged to increase from U_{-3} on the left-bottum corner to U_3 on the right-top corner like the boundary layer neighboring on the switching line. In a word, the linguistic rules of the simple FLC are arranged as a suction controller to have a switching line and a boundary layer. Thus, the simple FLC is termed a Fuzzy Suction Controller (FSC).

In the FSC, not only its linguistic rules, but also its characteristics are like a suction controller. The following Lemmas present this fact.

Lemma 1 (Tu *et al*., 2000): If

1. Its linguistic rules are designed as shown in Fig. 2,
2. The membership functions representing the fuzzy sets are a complement type (seeing Appendix B),

Then the FSC has a switching line

$$\hat{G}^T\hat{x} = G_1x_1 + G_2x_2 = 0 \tag{8}$$

Where G_1 and G_2 are the scaling factors to normalize E_e and E_c, respectively, and x_1 and x_2 are the input variables.

Note that x_1 and x_2 satisfy

$$G_1x_1=E_e \text{ and}$$

$$G_2x_2=E_c \tag{9}$$

The FSC is not only similar to a Sliding-Mode Controller (SMC), but also able to reduce chattering, which results from discontinuous control action. Although a quasi-SMC, termed suction controller, to suck the state vector into a boundary layer was proposed by Slotine (1984), it is difficult to determine a suitable boundary layer. Slotine (1984) used a linear function to approximate the boundary layer. The proposed FSC can change its boundary layer via the control action U_{-2}, ⋯, U_2 of Fig. 3. As a result, the FSC is more flexible for sucking the state vector within a boundary layer and avoiding chattering.

Lemma 2 (Tu *et al*., 2000): Let the output of the FSC be $F_{FLC}(\hat{x})$. Then, it can be approximated by

$$F_{FLC}(\hat{x}) = -G_u(\hat{G}^T\hat{x} + \text{sgn}(\hat{G}^T\hat{x})\delta) \tag{10}$$

where G_u is the de-normalized scaling factor, $\hat{G}^T\hat{x}$ is the switching line, and δ is the absolute value of the difference between the actual output and $\hat{G}^T\hat{x}$.

The FSC is the basic component of a MLFLC. Fig. 4 shows the scheme of the MISO system's MLFLC, namely the Γ. In Fig. 4, Γ is constructed

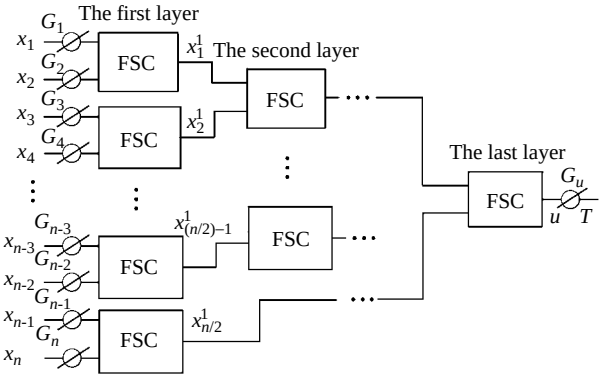

Fig. 4 The scheme of the MISO system's MLFLC, namely the Γ

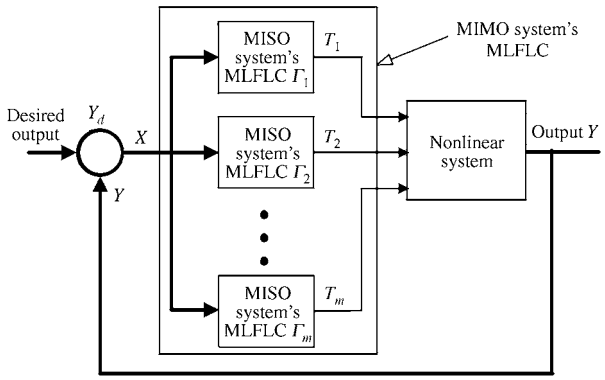

Fig. 5 The block diagram of MIMO system's MLFLC for a nonlinear system

with the sequence from the first layer to the last layer. The first layer plays the role of input and the last layer is used to produce a controller output. Except that the first layer has normalized scaling factors and the last layer has a de-normalized scaling factor, the other layers have no scaling factor. One layer is connected to the other layer directly, as shown in Fig. 4. Note that, in each layer, two inputs feed into one FSC and then this FSC output connects to the next layer. Thus, every layer in the FSC requires an even number of inputs. When numbers of inputs are odd in one layer, the last input of this layer is directly connected to the next layer. In Fig. 4, the second layer shows such a situation, $x_{n/2}^1$ is unconnected to the second layer and is directly connected to the third layer.

From Lemma 1, in the first layer of the MISO system's MLFLC, the FSCs have the following switching lines

$$G_1x_1+G_2x_2=0,$$

$$G_3x_3+G_4x_4=0, \cdots, \text{and}$$

$$G_{n-1}x_{n-1}+G_nx_n=0 \tag{11}$$

Similarly, the second layer FSCs have the following switching surfaces

$$G_1x_1+G_2x_2+G_3x_3+G_4x_4=0, \cdots, \text{and}$$

$$G_{n-5}x_{n-5}+G_{n-4}x_{n-4}+G_{n-3}x_{n-3}+G_{n-2}x_{n-2}=0 \tag{12}$$

Note that because x_{n-1} and x_n are directly connected to the third layer, they can not appear on Eq. (12). Therefore, in the last layer, the FSC has a switching surface

$$S=\overline{\boldsymbol{C}}^T\overline{x}$$

$$=G_1x_1+G_2x_2+G_3x_3+G_4x_4+\cdots+G_{n-3}x_{n-3}$$

$$+G_{n-2}x_{n-2}+G_{n-1}x_{n-1}+G_nx_n=0 \tag{13}$$

where $\overline{\boldsymbol{C}}^T=[G_1 \ G_2 \ \cdots \ G_{n-1} \ G_n]$. Thus, Γ has a switching surface as shown in Eq. (13).

Γ is the MISO system. For the MIMO system, many MISO systems' MLFLCs are composed to result in many outputs. Consider an m-input n-output system. The MLFLC needs m MISO systems to result in m outputs. This scheme, shown in Fig. 5, is the MIMO system's MLFLC designed for a MIMO nonlinear system. In Fig. 5, Γ_l (for l=1, ⋯, m) is the lth MISO system's MLFLC. Let the normalized scaling factors of Γ_l be $G_{l,j}$, for j=1, ⋯, n, and the de-normalized scaling factor of that be $G_{l,u}$. Then, similar to (13), Γ_l has a switching surface

$$S_l=\overline{\boldsymbol{C}}_l^T\overline{\boldsymbol{x}}$$

$$=G_{l,1}x_1+G_{l,2}x_2+G_{l,3}x_3+G_{l,4}x_4+\cdots+G_{l,n-3}x_{n-3}$$

$$+G_{l,n-2}x_{n-2}+G_{l,n-1}x_{n-1}+G_{l,n}x_n=0 \tag{14}$$

where $\overline{\boldsymbol{C}}_l^T=[G_{l,1} \ G_{l,2} \ \cdots \ G_{l,n-1} \ G_{l,n}]$ is the vector formed by the normalized scaling factors. In addition, there are m MISO system's MLFLCs (Γ_l, for l=1, ⋯, m.) in the MIMO system's MLFLC. Thus, m switching surfaces form the switching manifold in the MLFLC. Deriving from Eq. (14), the switching manifold is

$$\overline{\boldsymbol{S}}^T=[S_1 \ S_2 \ \cdots \ S_m]$$

$$=[\overline{\boldsymbol{C}}_0^T\overline{x}]^T=0, \tag{15}$$

where $\overline{\boldsymbol{C}}_0=[\overline{\boldsymbol{C}}_1 \ \overline{\boldsymbol{C}}_2 \ \cdots \ \overline{\boldsymbol{C}}_m]$, $\overline{\boldsymbol{C}}_l^T=[G_{l,1} \ G_{l,2} \ \cdots \ G_{l,n-1} \ G_{l,n}]$, for l=1, ⋯, m.

From Lemma 2, the output of the MISO system's MLFLC can be approximated by

$$T_l = -G_{l,u}(\overline{\boldsymbol{C}}_l^T \overline{\boldsymbol{x}} + \mathrm{sgn}(\overline{\boldsymbol{C}}_l^T \overline{\boldsymbol{x}})\delta_l) \quad (16)$$

where $G_{l,u}$ is the de-normalized scaling factor, and $\overline{\boldsymbol{C}}_l^T \overline{\boldsymbol{x}}$ is the switching surface. When the states are outside of the boundary, the output of Γ_l can be approximated by

$$\boldsymbol{T}^T = [\boldsymbol{T}_1 \ \ \boldsymbol{T}_2 \ \cdots \ \boldsymbol{T}_m] \quad (17)$$

where $\boldsymbol{T}_l = -(G_{l,u} - \delta_l)$, $\mathrm{sgn}(\overline{\boldsymbol{C}}_l^T \overline{x})$, for l=1, ⋯, m. Eq. (17) will be employed to study the stability of the MLFLC in the next section.

Equations (15) and (17) imply that the normalized and the de-normalized scaling factors are the main parameters of the MLFLC. Specifically, the de-normalized scaling factors can determine the bounded value of the MLFLC outputs, and the normalized scaling factors are the parameters of the switching manifold in the MLFLC. Traditional MIMO FLC design must consider many factors, such as fuzzy sets, membership functions, linguistic rules, and scaling factors, etc. Too many factors will result in complication of the FLC design. In contrast to traditional MIMO FLC design, the MLFLC only considers de-normalized and normalized scaling factors. Thus, the proposed MLFLC simplifies the MIMO FLC design procedures.

IV. STABILITY ANALYSIS

This section is devoted to discussing Problem 1. Note that although a three-link biped robot is a 3-inputs and 6-outputs system, the discussion of this section focuses on m-inputs and n-output systems, general MIMO systems.

Consider the nonlinear system described in Fig. 5 to be

$$\dot{\overline{\boldsymbol{Y}}} = \overline{\boldsymbol{F}}(\overline{\boldsymbol{Y}}) + \overline{\boldsymbol{G}}(\overline{\boldsymbol{Y}})\overline{\boldsymbol{T}} \quad (18)$$

where $\overline{\boldsymbol{Y}} \in R^n$ describes the system state, $\overline{\boldsymbol{F}}(\overline{\boldsymbol{Y}}) \in R^n$, $\overline{\boldsymbol{G}}(\overline{\boldsymbol{Y}}) \in R^{n\times m}$, and $\overline{\boldsymbol{T}} \in R^m$ are the control inputs. That is, the nonlinear system has m inputs and n outputs. For controlling the nonlinear system, the MLFLC needs the inputs to get the nonlinear system's outputs $\overline{\boldsymbol{Y}}$ minus the desired outputs $\overline{\boldsymbol{Y}}_d$. Thus, the MLFLC is designed to have n inputs, the same number as the outputs of the nonlinear system. Furthermore, the outputs of the MLFLC are used to control the nonlinear system for following the desired behavior. According to the number of the nonlinear system inputs, the outputs of the MLFLC are designed into m dimensions. Therefore, the MLFLC has an n-inputs and m outputs structure.

Let $\boldsymbol{Y}_{d,i}$ be the ith desired output, and $\boldsymbol{Y}_i$ be the ith actual output of the nonlinear system. Then, x_i, the input variable of the MLFLC, satisfies

$$x_i = \boldsymbol{Y}_i - \boldsymbol{Y}_{d,i}, \text{ for } i=1, \cdots, n.$$

Note that, after multiplied by the scaling factor $G_{l,i}$, x_i is connected to one FSC in the first layer.

In (18), we assume that every element of $\left\| \overline{\boldsymbol{C}}_0^T \overline{\boldsymbol{F}}(\overline{\boldsymbol{Y}}) \right\|$ is bounded over the range of operation conditions $\overline{\boldsymbol{Y}}$ and is known, and that the matrix $\overline{\boldsymbol{C}}_0^T \overline{\boldsymbol{G}}(\overline{\boldsymbol{Y}})$ is upper and lower bounded by

$$g_\ell \| \overline{\phi} \|^2 \le \overline{\phi}^T \overline{\boldsymbol{C}}_0^T \overline{\boldsymbol{G}}(\overline{\boldsymbol{Y}}) \overline{\phi} \le g_u \| \overline{\phi} \|^2 \quad (19)$$

where $g_\ell = \lambda_{\min}\{\overline{\boldsymbol{C}}_0^T \overline{\boldsymbol{G}}(\overline{\boldsymbol{Y}})\}$, $g_u = \lambda_{\max}\{\overline{\boldsymbol{C}}_0^T \overline{\boldsymbol{G}}(\overline{\boldsymbol{Y}})\}$, and an arbitrary vector $\overline{\phi} \in R^n$.

Lemma 3: With the controller Eq. (17), the dynamical system Eq. (18) is asymptotically stable if the following conditions are satisfied:

$$G_{l,u} > \frac{\|F_l\|}{g_\ell}, \text{ for } l=1, \cdots, m \quad (20)$$

where $G_{l,u}$ is the de-normalized scaling factor, $g_\ell = \lambda_{\min}\{\overline{\boldsymbol{C}}_0^T \overline{\boldsymbol{G}}(\overline{\boldsymbol{Y}})\}$, F_l is the lth element of $\left\| \overline{\boldsymbol{C}}_0^T \overline{\boldsymbol{F}}(\overline{\boldsymbol{Y}}) \right\|$.

Proof: Consider a Lyapunov function candidate,

$$V = \frac{1}{2}\overline{\boldsymbol{S}}^T \overline{\boldsymbol{S}} > 0$$

where $\overline{S}$ is the switching manifold.
Then,

$$\dot{V} = \overline{\boldsymbol{S}}^T \dot{\overline{\boldsymbol{S}}} \quad (21)$$

After some manipulation in (3) and substitution into (21) yields

$$\dot{V} = \overline{\boldsymbol{S}}^T [\overline{\boldsymbol{C}}_0^T \overline{\boldsymbol{F}}(\overline{\boldsymbol{Y}}) + \overline{\boldsymbol{C}}_0^T \boldsymbol{G}(\overline{\boldsymbol{Y}})\overline{\boldsymbol{T}}] \quad (22)$$

substituting (17) into (22) leads to

$$\begin{aligned} \dot{V} &= \overline{\boldsymbol{S}}^T [\overline{\boldsymbol{C}}_0^T \overline{\boldsymbol{F}}(\overline{\boldsymbol{Y}}) - \overline{\boldsymbol{C}}_0^T \boldsymbol{G}(\overline{\boldsymbol{Y}})[\boldsymbol{T}_1 \ \ \boldsymbol{T}_2 \ \cdots \ \boldsymbol{T}_m]^T] \\ &= \| \overline{\boldsymbol{S}} \| \sum_{l=1}^{m} (\|F_l\| - g_\ell G_{l,u} + \delta_l) \\ &\le \| \overline{\boldsymbol{S}} \| \sum_{l=1}^{m} (\|F_l\| - g_\ell G_{l,u}) \end{aligned} \quad (23)$$

If (20) is satisfied, then we have

$$\dot{V} < 0.$$

Therefore, the system is asymptotically stable.

Remark 1: Lemma 3 solves Problem 1. In addition, it shows that the de-normalized scaling factors in the MLFLC can be used to stabilize the MIMO systems.

V. DESIGN OF NORMALIZED SCALING FACTORS VIA POLE ASSIGNMENT

The MLFLC design simplifies MIMO FLC into only a choice of de-normalized and normalized scaling factors. It has been shown that the de-normalized scaling factor is related to the system stability condition. In this section, emphasis will be on the normalized scaling factors.

The design of normalized scaling factors will be started by constructing a switching manifold. This is because after this is constructed, normalized scaling factors can be determined from Eq. (15). A switching manifold is an important design issue for a system under sliding mode control. When a system enters the sliding mode, its states go toward the origin along the switching manifold, and its dynamic behavior can then be approached through the switching manifold. The sliding mode control can be viewed as controlling a system dynamics to approach a switching manifold. In our previous paper (Lee *et al*., 1997), it was shown that the slope of the switching line could be used to achieve a faster rise time. Such ideas can also be implemented by pole locations if the switching line is viewed as the characteristic function of a control system. Reconsidering Eq. (8). If

$x_1=x$, and

$$x_2=\frac{dx}{dt},$$

then Eq. (8) becomes

$$G_1x+G_2\frac{dx}{dt}=0 \tag{24}$$

After the Lapace transformation, Eq. (24) can be rewritten as

$$(G_1+G_2\vartheta)X(\vartheta)=0 \tag{25}$$

The pole of the above equation is $-G_1/G_2$. Usually, $G_1>0$ and $G_2>0$ are such that the pole locates at the left-half complex domain to ensure system stability. Besides, the pole will result in a fast time response as its location is far away from the origin, while the pole will result in a slow time response as it becomes nearer to the origin. As a result, the pole location derived from a switching line can be used to pursue the system time response requirement. Thus, the characteristic function, which is formed by the assigned pole locations, can be used to design a switching line. Similarly, a switching manifold in a MLFLC can be designed by assigning pole locations. The details are shown below.

The n-inputs m-outputs MLFLC must contain m MISO systems' MLFLC Γ_l, for l=1, ⋯, m. Γ_l has a switching surface S_l. Thus, m switching surfaces form a switching manifold. In addition, because the MLFLC has n inputs, the lth switching surface S_l, viewed as characteristic function $\Im_l$, is a polynomial of degree $n-1$. Thus, $n-1$ poles exist in $\Im$ for S_l. Let

$$\Im_l=\prod_{i=1}^{n-1}(\vartheta+\gamma_{l,i}) \tag{26}$$

where $\gamma_{l,i}$ (for i=1, ⋯, ($n-1$)) is the pole of the characteristic function. Eq. (26) can be rewritten as

$$\Im_l=\sum_{k=0}^{n-1}(-1)^k a_k(\gamma_{l,1},\cdots,\gamma_{l,n-1})\vartheta^{n-1-k} \tag{27}$$

where a_0=1 and

$$a_k(\gamma_{l,1},\cdots,\gamma_{l,n-1})\equiv\sum_{1\le i_1<\cdots<i_k\le(n-1)}\prod_{j=1}^{k}\gamma_{l,i_j} \tag{28}$$

for k=1, ⋯, $n-1$, is the sum of all k-fold $\binom{n-1}{k}$ products of distinct items from $\gamma_{l,1}$, ⋯, $\gamma_{l,n-1}$. For example:

$$a_1(\gamma_{l,1},\cdots,\gamma_{l,n-1})=\gamma_{l,1}+\gamma_{l,2}+\cdots+\gamma_{l,n-1}$$

$$\vdots$$

$$a_{n-1}(\gamma_{l,1},\cdots,\gamma_{l,n-1})=\gamma_{l,1}\gamma_{l,2}\cdots\gamma_{l,n-1}$$

In summary, $\gamma_{l,i}$ (for i=1, ⋯, ($n-1$)) are used to construct the switching surface S_l. All switching surfaces (S_l for l=1, ⋯, m) are constructed to consist of the switching manifold in the MLFLC.

After constructing the switching manifold, normalized scaling factors are determined from Eq. (15). In other words, normalized scaling factors are designed such that an MLFLC has the desired switching manifold. In order to let a switching manifold have one switching surface S_l as shown in Eq. (15), a_k ($\gamma_{l,1}$, ⋯, $\gamma_{l,n-1}$), for k=1, ⋯, $n-1$, are the base of design of normalized scaling factors. The detail will be described in the next section.

VI. MLFLC DESIGN FOR THE THREE-LINK BIPED ROBOT

Assigning pole locations for selecting normalized scaling factors is illustrated by the MLFLC control system design for a three-link biped robot. The illustration is divided into two parts. The first part is used to illustrate how to design the MLFLC for achieving faster time response and smaller PI. The

second part reveals the MLFLC can control the biped walking at varying speed. Note that these two parts are used to solve Problem 2 and Problem 3, respectively.

1. Design for Better Performance Requirement

The key design point of an MLFLC is to choose suitable normalized and de-normalized scaling factors for respectively satisfying performance requirements and stability of the biped system. As pointed out in section IV and section V, the de-normalized scaling factors are chosen to satisfy the system stability conditions and the normalized scaling factors are the switching manifold parameters, determined by pole locations in the biped system. As shown in Eqs (20) and (23), the system stability conditions are expressed in terms of the switching manifold parameters, the normalized scaling factors. Thus, the MLFLC design will begin with the choice of normalized scaling factors.

For a three-link biped system, the MLFLC requires three outputs to control its links. Thus, there are three switching surfaces, S_1, S_2 and S_3 to form a switching manifold. In addition, the three-link biped robot is a six-order system. Therefore, five poles are need for the switching surface design in the MLFLC. Let the five poles be -0.2, -5+5i, -5-5i, 4.8+5i, and 4.8-5i. Then, the characteristic function is

$$\vartheta^5+0.6\vartheta^4+2.1\vartheta^3+0.8\vartheta^2+2402.1\vartheta+480.4=0 \tag{29}$$

where ϑ is the variable resulting from the Laplace transform. After being multiplied by 1/62.8, Eq. (29) becomes

$$\frac{1}{62.8}\vartheta^5+\frac{0.6}{62.8}\vartheta^4+\frac{2.1}{62.8}\vartheta^3+\frac{0.8}{62.8}\vartheta^2+\frac{2402.1}{62.8}\vartheta+\frac{480.4}{62.8}=0 \tag{30}$$

The coefficients of Eq. (30) are used to choose the proper parameters for the switching surfaces, the scaling factors $G_{i,1}$, $G_{i,2}$, $G_{i,3}$, $G_{i,4}$, $G_{i,5}$, and $G_{i,6}$, for i=1, ···, 3. Note that Eq. (30) multiplied by 1/62.8 will form the boundary distance between one switching surface and the boundary layer. The detailed description of the boundary distance can be found in Lee *et al*. (1997).

It is unknown which coefficients in Eq. (30) will be assigned to which normalized scaling factors to form a switching surface. This question can be solved by considering the action of the scaling factors to the FLC. In general, a larger scaling factor enlarges the action of its input on the FLC, while a smaller one reduces its action. Because the switching surface S_1,

$$G_{1,1}x_1+G_{1,2}\dot{x}_1+G_{1,3}x_2+G_{1,4}\dot{x}_2+G_{1,5}\dot{x}_3+G_{1,6}\dot{x}_3=0,$$

is used to produce the controller output for T_1, x_1 and $\dot{x}_1$ are the main variables of the controller input. Hence, the larger coefficients $\frac{480.4}{62.8}$ and $\frac{2402.1}{62.8}$ respectively are assigned to $G_{1,1}$ and $G_{1,2}$ for enlarging the action of x_1 and $\dot{x}_1$ on T_1. For the rest,

$$G_{1,3}=\frac{0.8}{62.8},\ G_{1,4}=\frac{2.1}{62.8},\ G_{1,5}=\frac{0.6}{62.8},\ \text{and}$$

$$G_{1,6}=\frac{1.0}{62.8}.$$

For simplicity, the three switching surfaces of the switching manifold are formed by S_1. That is, Eq. (30) is also used to determine the parameters of the switching surfaces S_2 and S_3. Similarly, for S_2,

$$G_{2,1}=\frac{0.6}{62.8},\ G_{2,2}=\frac{1.0}{62.8},\ G_{2,3}=\frac{480.4}{62.8},$$

$$G_{2,4}=\frac{2402.1}{62.8},\ G_{2,5}=\frac{0.8}{62.8},\ G_{2,3}=\frac{2.1}{62.8},$$

and for S_3,

$$G_{3,1}=\frac{0.8}{62.8},\ G_{3,2}=\frac{2.1}{62.8},\ G_{3,3}=\frac{0.6}{62.8},$$

$$G_{3,4}=\frac{1}{62.8},\ G_{3,5}=\frac{480.4}{62.8},\ G_{3,6}=\frac{2402.1}{62.8},$$

After the normalized scaling factors are chosen, the de-normalized scaling factors can be selected by $G_{1,u}$=1500, $G_{2,u}$=1000 and $G_{3,u}$=1500 to satisfy Eq. (20). In Fig. 6, the dash-dot line is the simulation

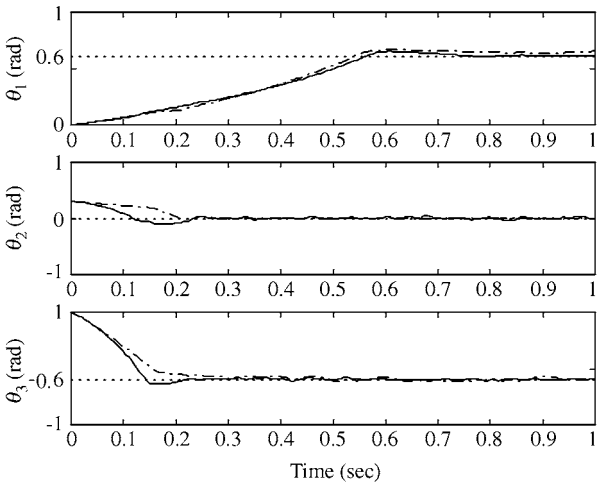

Fig. 6 The comparison of the time responses among the different switching surfaces

Table 2 Comparison of the simulation results due to different poles

One different pole	PI	Rise time of θ_1	Rise time of θ_2	Rise time of θ_3
-0.2	0.0027	0.575	0.21	0.21
-1.0	0.0024	0.575	0.115	0.13

result of the time response during biped walking from the left-leg support phase to the double support phase. Note that, for simplicity, let Q and R of Eq. (4) be identity matrices $I_{6\times6}$ and $I_{3\times3}$, respectively. Then the defined performance index PI is equal to 0.0027.

When the five poles are changed into -1, -5+5i, -5-5i, 4.8+5i, and 4.8-5i, Eq. (30) becomes

$$\frac{1}{62.8}\vartheta^5 + \frac{1.6}{62.8}\vartheta^4 + \frac{2.5}{62.8}\vartheta^3 + \frac{2.8}{62.8}\vartheta^2 + \frac{2402.5}{62.8}\vartheta + \frac{2882.4}{62.8} = 0 \quad (31)$$

Thus, the normalized scaling factors can be

$$G_{1,1} = \frac{2882.4}{62.8},\ G_{1,2} = \frac{2402.5}{62.8},\ G_{1,3} = \frac{2.5}{62.8},$$

$$G_{1,4} = \frac{2.8}{62.8},\ G_{1,5} = \frac{1.6}{62.8},\ G_{2,3} = \frac{1}{62.8},$$

$$G_{2,1} = \frac{1.6}{62.8},\ G_{2,2} = \frac{1}{62.8},\ G_{2,3} = \frac{2882.4}{62.8},$$

$$G_{2,4} = \frac{2402.5}{62.8},\ G_{2,5} = \frac{2.5}{62.8},\ G_{2,3} = \frac{2.8}{62.8},$$

and

$$G_{3,1} = \frac{2.5}{62.8},\ G_{3,2} = \frac{2.8}{62.8},\ G_{3,3} = \frac{1.6}{62.8},$$

$$G_{3,4} = \frac{1}{62.8},\ G_{3,5} = \frac{2882.4}{62.8},\ G_{3,6} = \frac{2402.5}{62.8}.$$

In Fig. 6, the solid line shows the time response of the biped walking from the left-leg support phase to the double support phase. In addition, PI=0.0024.

Remark 2: The above two cases show the results of one different pole changed from -0.2 to -1.0. Simulation results are compared in Table 2.

Table 2 reveals that the when pole location is changed from -0.2 to -1.0, the biped system achieves faster time response and smaller PI. This fact solves Problem 2.

2. Design for Biped Walking at Varying Speeds

The study is under the assumption that the biped robot walks only in single-support phase. Thus, in the simulation of biped walking, one single-support phase ends after the swing leg touches on the ground. And then the biped robot begins with the other single-support phase.

The biped robot is controlled to follow a desired walking pattern for walk. In this research, Eqs. (5) – (7) are the desired walking pattern. When the five poles are chosen as -0.1794, -3+5i, -3-5i, 3+5i, and 3-5i, Eq. (30) becomes

$$\frac{1}{62.8}\vartheta^5 + \frac{0.2}{62.8}\vartheta^4 + \frac{32}{62.8}\vartheta^3 + \frac{5.7}{62.8}\vartheta^2 + \frac{1156}{62.8}\vartheta + \frac{207.4}{62.8} = 0$$

Thus, the normalized scaling factors are selected as

$$G_{1,1} = \frac{207.4}{62.8},\ G_{1,2} = \frac{1156}{62.8},\ G_{1,3} = \frac{5.7}{62.8},$$

$$G_{1,4} = \frac{32}{62.8},\ G_{1,5} = \frac{0.2}{62.8},\ G_{2,3} = \frac{1}{62.8},$$

$$G_{2,1} = \frac{0.2}{62.8},\ G_{2,2} = \frac{1}{62.8},\ G_{2,3} = \frac{207.4}{62.8},$$

$$G_{2,4} = \frac{1156}{62.8},\ G_{2,5} = \frac{5.7}{62.8},\ G_{2,3} = \frac{3.2}{62.8},$$

and

$$G_{3,1} = \frac{5.7}{62.8},\ G_{3,2} = \frac{32}{62.8},\ G_{3,3} = \frac{0.2}{62.8},$$

$$G_{3,4} = \frac{1}{62.8},\ G_{3,5} = \frac{207.4}{62.8},\ G_{3,6} = \frac{1156}{62.8}.$$

Figure 7 shows the simulation result for every joint to track its desired trajectory with large error. The stick diagram of the biped walking is shown in Fig. 8. It is obvious that the biped cannot perform every single-support phase completely because the swing leg touches on the ground too early. This is bad or inefficient walking.

When the five poles are changed into -0.1794, -6+5i, -6-5i, 6+5i, and 6-5i, Eq. (30) becomes

$$\frac{1}{62.8}\vartheta^5 + \frac{0.2}{62.8}\vartheta^4 - \frac{22}{62.8}\vartheta^3 - \frac{3.9}{62.8}\vartheta^2 + \frac{3721}{62.8}\vartheta + \frac{667.5}{62.8} = 0$$

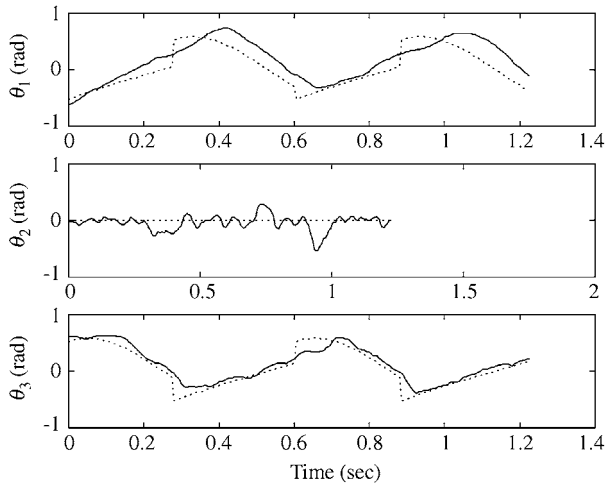

Fig. 7 The joint trajectories of the biped robot controlled for tracking the desired trajectories: the case of a large tracking error (the dotted line is desired and the solid line is actual)

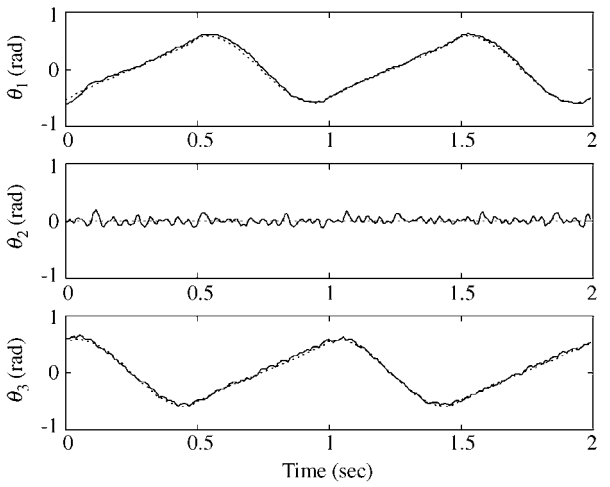

Fig. 9 The joint trajectories of the biped robot controlled for tracking the desired trajectories: the case of a small tracking error (the dotted line is desired and solid line is actual)

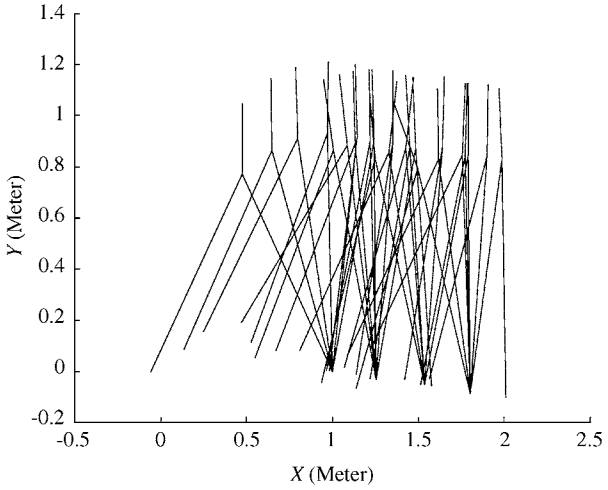

Fig. 8 The height of the biped robot is descending gradually

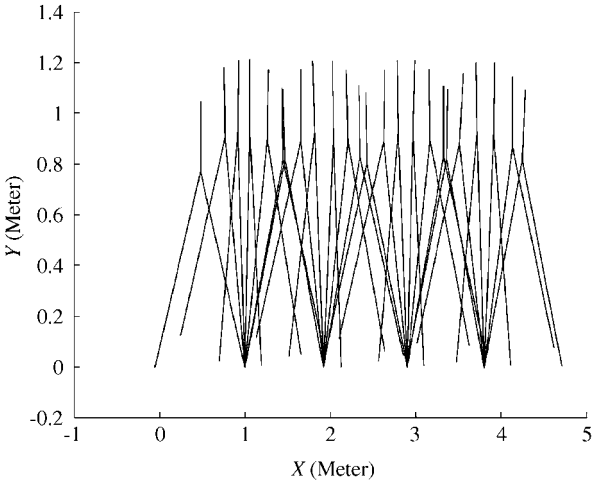

Fig. 10 The stick diagram: the biped robot controlled to maintain the same height between walking cycles

Thus, the normalized scaling factors can be assigned as

$$G_{1,1}=\frac{667.5}{62.8},\ G_{1,2}=\frac{3721}{62.8},\ G_{1,3}=\frac{-3.9}{62.8},$$

$$G_{1,4}=\frac{-22}{62.8},\ G_{1,5}=\frac{0.2}{62.8},\ G_{2,3}=\frac{1}{62.8},$$

$$G_{2,1}=\frac{0.2}{62.8},\ G_{2,2}=\frac{1}{62.8},\ G_{2,3}=\frac{667.5}{62.8},$$

$$G_{2,4}=\frac{3721}{62.8},\ G_{2,5}=\frac{-3.9}{62.8},\ G_{2,3}=\frac{-22}{62.8},$$

and

$$G_{3,1}=\frac{-3.9}{62.8},\ G_{3,2}=\frac{-22}{62.8},\ G_{3,3}=\frac{0.2}{62.8},$$

$$G_{3,4}=\frac{1}{62.8},\ G_{3,5}=\frac{667.5}{62.8},\ G_{3,6}=\frac{3721}{62.8}.$$

Fig. 9 shows both the actual and the desired trajectories of the biped robot. Fig. 10 shows the stick diagram of the biped robot, and shows it repeating the walking cycle. The biped robot is under control and performs walks perfectly. Figs. 7 – 10 show that the pole locations can be designed to vary the normalized scaling factors to achieve better biped walking performance.

When a biped robot is walking, its controller must overcome the impact effects, the reactive force from the ground. To demonstrate the robustness of the proposed MLFLC, Figs. 11 and 12 show that the biped walking can tolerate a reactive force of 3 kg

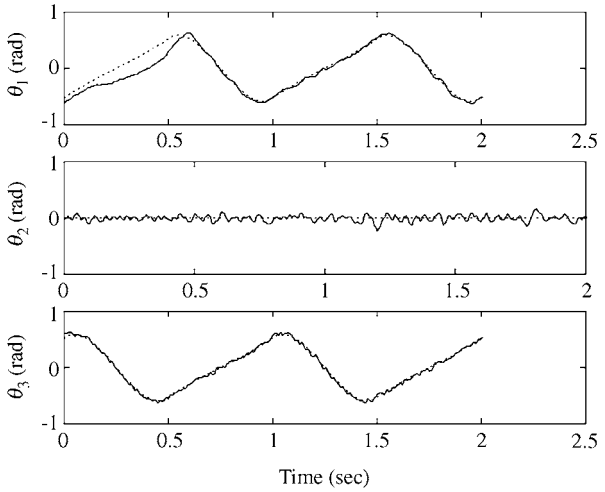

Fig. 11 The joint trajectories of the biped robot bearing the impact effect of 3 kg

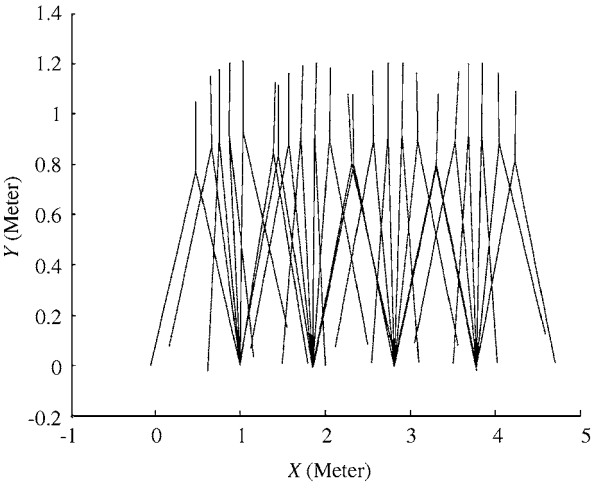

Fig. 12 The stick diagram as the biped walking bears 3kg impact effect

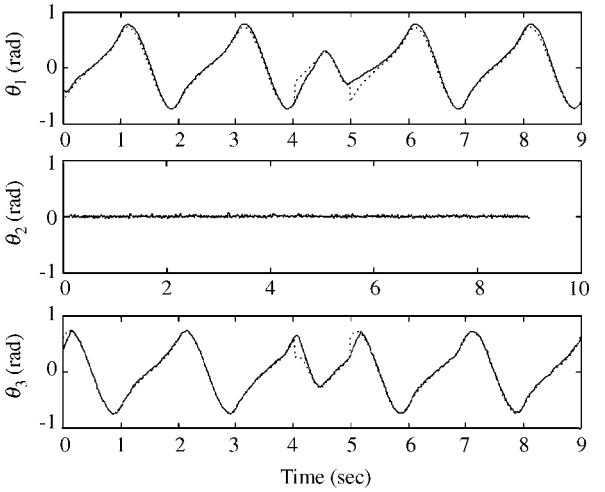

Fig. 13 The joint trajectories of the biped controlled for varying the walking speed (the dot line is desired and solid line is actual)

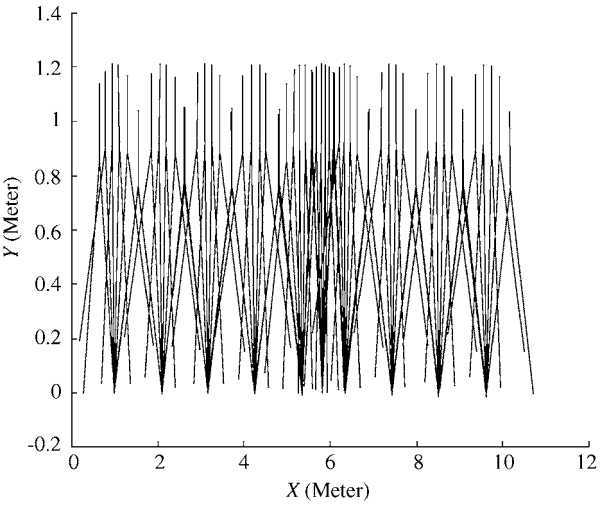

Fig. 14 The stick diagram of the biped walking during speed variations

due to its sole touching the ground.

Finally, this MLFLC is used to control the biped for varying speeds. The controlled trajectories are shown in Fig. 13. The gait speed of the biped walking is θ_m=35° and T_m=1.0, but is changed θ_m=15° and T_m=0.5 during the time between 4 and 6 seconds. Fig. 14 shows a corresponding stick diagram of the biped walking. Fig. 13 and Fig. 14 show that the MLFLC can control the biped walking system at varying speeds.

VII. CONCLUSIONS

This paper addresses the application of a Multi-Layer Fuzzy Logic Control (MLFLC) for controlling a three-link biped robot at varying walking speeds. It is shown that closed-loop pole locations, and hence characteristic equations, are related to normalized scaling factors. Due to different pole locations, the normalized scaling factors can be adjusted to achieve a satisfactory time response and to control a biped walking robot at varying speeds. When a biped robot needs to change its walking speed, the MLFLC provides for stable control during change. In addition, the de-normalized scaling factors of the MLFLC can be designed for ensuring the system stability. The proposed MLFLC is able to reduce the design procedure of the MIMO FLCs into selecting only the normalized and de-normalized scaling factors. Thus, the MLFLC simplifies the MIMO FLC design for better performance.

ACKNOWLEDGMENTS

This research was supported by National

Science Council, Taiwan, Rep. of China under Grants NSC-89-2218-E-146-003 and NSC-89-2218-E-146-005.

NOMENCLATURE

a_k	the parameters of the characteristic function
$\tilde{A}_i$, $\tilde{B}_i$	fuzzy sets
$\overline{\boldsymbol{C}}^T$	the vector of normalized scaling factors, i.e., $[G_1\ G_2 \cdots G_n]$
E_e, E_c	the normalized scaling factors of a FLC
$\overline{f}(\overline{\theta}, \dot{\overline{\theta}})$	the centripetal, coriolis and gravitational effect in dynamical equation of a three-link biped robot
FLC	fuzzy logic controllers
g_l	the minimal eigenvalue of $\overline{\boldsymbol{C}}_0^T \overline{G}(\overline{Y})$
g_u	the maximal eigenvalue of $\overline{\boldsymbol{C}}_0^T \overline{G}(\overline{Y})$
G_j	the normalized scaling factors of an MLFLC
$G_{l,j}$	the normalizing scaling factors of the *l*th MISO system's MLFLC
$G_{l,u}$	the de-normalizing scaling factor of the *l*th MISO system's MLFLC
G_u	the de-normalized scaling factor of a FLC
MIMO	multi-input multi-output
MISO	multi-input single-output
MLFLC	a multi-layer fuzzy logic controller
$\overline{\boldsymbol{M}}(\overline{\theta})$	the inertia or mass matrix in dynamical equation of a three-link biped robot
$\overline{\boldsymbol{N}}$	the input matrix in dynamical equation of a three-link biped robot
P_i, D_j	the parameters of the planned trajectories of the joint angles of the three-link biped robot (for i=1, ⋯, 4, and j=1,2.)
S_l	the switching surface formed by the *l*th MISO system's MLFLC
T_l	the output of the *l*th MISO system's MLFLC
$\overline{\boldsymbol{T}}$	the input vector in dynamic equation of a three-link biped robot
T_m	the period of a single-support phase
U_i	the control action of a FLC
x_i	the input variable of the MLFLC, i. e., the difference between Y_i and $Y_{d,i}$
$\overline{\boldsymbol{Y}}$	the system states of a nonlinear system
$\overline{\boldsymbol{Y}}_d$	the desired states of a nonlinear system
$\gamma_{l,i}$	the pole of the characteristic function used to design a MLFLC
θ_1^*, θ_2^*, θ_3^*	the planned trajectories of the joint angles of the three-link biped robot
θ_m	the maximal swing angle between the leg and the vertical in the sagittal plane
$\dot{\overline{\boldsymbol{\theta}}}$	the velocity vector of the joint angles of a three-link biped robot
$\ddot{\overline{\boldsymbol{\theta}}}$	the acceleration vector of the joint angles of a three-link biped robot
$\Im_l$	the characteristic function used to design a MLFLC

REFERENCES

Arimoto, S., and Miyazaki, F., 1984, "Biped Locomotion Robots," *Computer Science & Technologies*, T. Kitagawa ed., North-Holland, Amsterdam, The Netherlands, Chapter 2, pp. 194-205.

Borovac, B., Vukobratovic, M., and Surla, D., 1989, "An Approach to Biped Control Synthesis," *Robotica*, Vol. 7, No. 3, pp. 231-241.

Frank, A. A., 1970, "An Approach to the Dynamic Analysis and Synthesis of Biped Locomotion Machines," *Medical Biological Engineering*, Vol. 8, pp. 465-476.

Frank, A. A., and Vukobratovic, M., 1979, "On the Gait Stability of Biped Machine," *IEEE Transactions on Automatic Control*, Vol. 15, No. 6, pp. 678-679.

Furusho, J., and Sano, A., 1990, "Sensor-Based-Control of a Nine Link Biped," *International Journal of Robotic Research*, Vol. 9, No. 2, pp. 83-98.

Grishin, A. A., Formalsky, A. M., Lensky, A. V., and Zhitomirsky, S. V., 1994, "Dynamic Walking of a Vehicle with Two Telescopic Legs Controlled by Two Drivers," *International Journal of Robotic Research*, Vol. 13, No. 2, pp. 137-147.

Gubina, F., Hemami, H., and McGhee, R. B., 1974, "On the Dynamic Stability of Biped Locomotion," *IEEE Transactions on Biomedical Engineering*, Vol. 21, No. 2, pp. 102-108.

Hemami, H., and Wyman, B. F., 1979, "Modeling and Control of Constrained Dynamic Systems with Application to Biped Locomotion in the Frontal Plane," *IEEE Transactions on Automatic Control*, Vol. 24, No. 4, pp. 526-535.

Hodgins, J. K., and Raibert, M. H., 1991, "Adjusting Step Length for Rough Terrain Locomotion," *IEEE Transactions on Robotics and Automation*, Vol. 7, No. 3, pp.289-298.

Kajita, S., Yamaura, T., and Kobayashi, A., 1992, "Dynamic Walking Control of a Biped Robot along a Potential Energy Conserving Orbit," *IEEE Transactions on Robotics and Automation*, Vol. 8, No. 4, pp. 431-438.

Kato, I., Ohteru, S., Kobayashi, H., Shrai, K., and Uchiyama, A., 1974, "Information-Power Machine with Sense and Climbs," *Proceedings of the 1st CISM-IFToMM Symposium On Theory And Practice of Robots and Manipulation*, Springer-Verlag, Berlin, Germany.

Kum, A. L., and Miller, III, W. T., 1999, "Control of Variable-Speed Gaits for a Biped Robot," *IEEE*

Robotics and Automation Magazine, Vol. 6, No. 3, pp. 19-29.

Lee, T. T., and Liao, J. H., 1988, "Trajectory Planning and Control of a 3-link Biped Robot," Proceedings of the *IEEE International Conference on Robotics and Automation*, Philadelphia, PA, USA, Vol. 2, pp. 820-823.

Lee, T. T., Tu, K. Y., and Wang, W. J., 1997, "Design of a Fuzzy Logic Controller as a Suction Controller," *Fuzzy Sets and Systems*, Vol. 91, No. 3, pp. 305-317.

Miller, W. T., 1994, "Real-Time Neural Network Control of a Biped Walking Robot," *IEEE Control Systems magazine*, Vol. 14, No. 1, pp. 41-48.

Minakata, H., and Hori, Y., 1994, "Realtime Speed-Changeable Biped Working by Controlling the Parameter of Virtual Inverted Pendulum," *IEEE IECON'94*, Bologna, Italy, pp. 1009-1014.

Miura, H., and Shimoyama, H., 1984, "Dynamic Walk of Biped Locomotion," *International Journal of Robotics Research*, Vol. 3, No. 2, pp. 60-74.

Raibert, M. H., 1986, *Legged Robots That Balance*, MIT Press, Cambridge, MA, USA.

Shih, C.-L., and Chiou, C.-J., 1998, "The Motion Control of a Statically Stable Biped Robot on an Uneven Floor," *IEEE Transactions on Systems, Man, and Cybernetics*, Part B: Cybernetics, Vol. 28, No. 2, pp. 244-249.

Shih, C.-L., and Gruver, W. A., 1992, "Control of a Biped Robot in the Double-support Phase," *IEEE Transactions on Systems, Man and Cybernetics*, Vol. 22, No. 4, pp. 729-735.

Slotine, J-T. E., 1984, "Sliding Controller Design for Nonlinear Systems," *International Journal of Control*, Vol. 40, No. 2, pp. 421-434.

Song, S. M., and Waldron, K. J., 1988, *Machines That Walk: The Adaptive Suspension Vehicle*, MIT Press, Cambridge, MA, USA.

Takanishi, A., Ishida, M., Yamazaki, Y., and Kato, I., 1985,"The Realization of Dynamic Walking by Biped Walking Robot WL-10RD," *Proceedings of the International Conference on Advanced Robotics*, Tokyo, Japan, pp. 459-466.

Tu, K. Y., Lee, T. T., and Wang, W. J., 2000, "Design of a Multi-Layer Fuzzy Logic Controller for Multi-Input Multi-Output Systems," *Fuzzy Sets and Systems*, Vol. 111, No. 3, pp. 199-214.

Vukobratovic, M., Frank, A. A., and Juricic, D., 1970, "On the Stability of Biped Locomotion," *IEEE Transactions on Biomedical Engineering*, Vol. 17, No. 1, pp. 25-36.

Zheng, Y. F., and Shen, J., 1990, "Gait Synthesis for the SD-2 Biped Robot to Climb Sloping Surface," *IEEE Transactions on Robotics and Automation*, Vol. 6, No. 1, pp. 86-96.

Zheng, Y. F., and Sias. Jr., F. R., 1988, "Design and Motion Control of Practical Biped Robots," *International Journal of Robotics and Automation*, Vol. 3, No. 2, pp. 70-77.

Manuscript Received: Aug. 28, 2002
Revision Received: Mar. 10, 2003
and Accepted: Apr. 18, 2003

APPENDIX A

In the sagittal plane, the dynamical equation for the biped as shown in Fig. 1 is

$$\overline{\boldsymbol{M}}(\overline{\boldsymbol{\theta}},\dot{\overline{\boldsymbol{\theta}}})\ddot{\overline{\boldsymbol{\theta}}}=\overline{\boldsymbol{f}}(\overline{\theta},\dot{\overline{\theta}})+\overline{\boldsymbol{N}}\overline{\boldsymbol{T}} \tag{A1}$$

where $\ddot{\overline{\boldsymbol{\theta}}}=[\ddot{\theta}_1\ \ddot{\theta}_2\ \ddot{\theta}_3]^T$, $\overline{\boldsymbol{T}}=[T_1\ T_2\ T_3]^T$, $\overline{M}(\cdot)$ and $\overline{\boldsymbol{N}}$ are the matrices of 3×3, and $\overline{f}(\cdot)$ is the column vector of 3×1. The elements of $\overline{M}(\cdot)$ are

$$M_{11}=1$$

$$M_{12}=-\alpha_{12}\cos(\theta_1+\theta_2)$$

$$M_{13}=0$$

$$M_{21}=\alpha_2\cos(\theta_2-\theta_1)$$

$$M_{22}=1$$

$$M_{23}=0$$

$$M_{31}=\alpha_3\cos(\theta_3-\theta_1)$$

$$M_{32}=0$$

$$M_{33}=1$$

where

$$\alpha_{12}=m_2\ell_1\ell_2/\Delta_1$$

$$\alpha_{13}=m_3\ell_1\ell_{a3}/\Delta_1$$

$$\Delta_1=m_1\ell_{a1}^2+I_{1s}-2m_1\ell_1\ell_{a1}+(m_1+m_2+m_3)\ell_1^2$$

$$\alpha_2=m_2\ell_1\ell_2/\Delta_2$$

$$\Delta_2=m_1\ell_2^2+I_{2s}$$

$$\alpha_{13}=m_3\ell_1\ell_{a3}/\Delta_3$$

$$\Delta_3=m_1\ell_{a3}^2+I_{3s}$$

The elements of the column vector $\overline{f}(\cdot)$ are

$$f_1=\alpha_{12}\dot{\theta}_1^2\sin(\theta_1-\theta_2)+\alpha_{13}\dot{\theta}_3^2[\cos(\theta_1-\theta_2)+\sin(\theta_1-\theta_2)]+\beta_1\sin\theta_1$$

$$f_2 = -\alpha_2\dot{\theta}_1^2\sin(\theta_2-\theta_1)+\beta_2\sin\theta_2$$

$$f_3 = \alpha_3\dot{\theta}_1^2\sin(\theta_3-\theta_1)-\beta_3\sin\theta_3$$

where

$$\beta_1=[(m_1+m_2+m_3)g\ell_1-m_1g\ell_{a1}]/\Delta_1$$

$$\beta_2=m_2\ell_2 g/\Delta_2$$

$$\beta_3=m_3\ell_{a3}g/\Delta_3$$

The matrix $\overline{N}$ are

$$\begin{bmatrix} \gamma_1 & -\gamma_1 & 0 \\ 0 & \gamma_2 & \gamma_2 \\ 0 & 0 & -\gamma_3 \end{bmatrix}$$

where

$$\gamma_1=1/\Delta_1$$

$$\gamma_2=1/\Delta_2$$

$$\gamma_3=1/\Delta_3$$

Note that m_1, m_2 and m_3 are the masses of the links, respectively, ℓ_1, ℓ_2 and ℓ_3 are the lengths of the links, respectively, I_{1s}, I_{2s} and I_{3s} are the inertias of the links, respectively, and ℓ_{ai} is the distance between the center of mass of link i (for i=1, 2, and 3) and the hip.

APPENDIX B

Definition 1: The membership functions in a term set are of a complement type if the following conditions hold

i) The space between two adjacent central values A_i' of fuzzy set $\tilde{A}_i$ is equal,

ii) The membership functions of all fuzzy sets are the same form,

iii) Corresponding to one support value E_1 in the linguistic variable E, there are two membership grades $\mu_{\tilde{A}_i}$ and $\mu_{\tilde{A}_{i+1}}$ which satisfy

$$\mu_{\tilde{A}_i}(E_1) = 1-\mu_{\tilde{A}_{i+1}}(E_1)$$